PYROXENE RELATIONS IN HIGHLAND PLUTONIC AND HIGH GRADE METAMORPHIC ROCKS, I. S. McCallum, F.P. Okamura, E. A. Mathez, and S. Ghose, Department of Geological Sciences, University of Washington, Seattle, Washington, 98195

67075 is an extremely friable anorthositic breccia from Station 11, North Ray Crater, composed of over 80% anorthitic plagioclase, which occurs as isolated fragments and as micro-anorthosites with polygonal grain boundaries. Mafic minerals include pyroxene, showing unusually well developed exsolution lamellae up to 30 μm wide, olivine, Ti-chromite, ilmenite, Fe-Ni, and troilite. Single crystal x-ray precession photographs reveal a very complex pattern of multiple exsolution and inversion in the pyroxene grains (Fig. 1). Cell dimensions of the components in two selected crystals are given in Table 1, and probe analyses are listed in Table 2. While host and exsolved phases in individual macrocrystals are homogeneous, considerable intergrain variation exists. The Ca contents and K_D (Fe-Mg) values of adjacent host-lamellae pairs indicate extensive subsolidus, "intracrystalline" reequilibration. Pigeonite has exsolved augite on (001) and (100) planes. Diffuse streaks parallel to a* connect host pigeonite reflections to corresponding hypersthene reflections, indicating partial inversion. This inversion is isochemical and probably occurs metastably. Splitting of the c* axes (Δc^*) of pigeonite and augite sharing (001) permits identification of second generation exsolution lamellae. Second generation pigeonite has not inverted. Augite macrocrystals exsolved several sets of clinohypersthene lamellae on both (001) and (100) planes. Diffuse streaks parallel to a* extend from the (001)-clinohypersthene reflections and show intensity maxima at positions expected for hypersthene reflections, indicating incipient inversion. An estimate of the extent of the inversion together with the magnitude of Δc^* and $\Delta\beta$ serves as a qualitative indicator of the cooling rate. Comparative studies show that 67075 pyroxenes cooled more slowly than Skaergaard pyroxene (EG 4430) and more rapidly than Stillwater pyroxene (M-50) (Fig. 1). On the basis of features observed in pyroxenes of 67075, we infer an origin in a deep seated magma chamber (5-10 km) which existed during the formation of the primitive lunar crust.

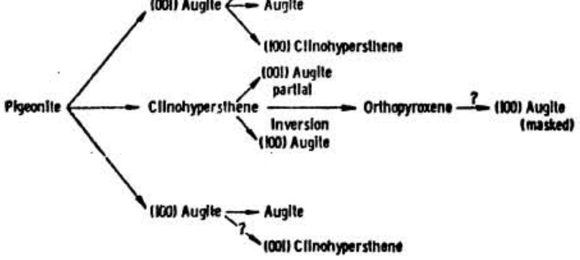

Fig. 1a. Schematic diagram outlining the exsolution and inversion phenomena in 67075, 18, 1 pigeonite.

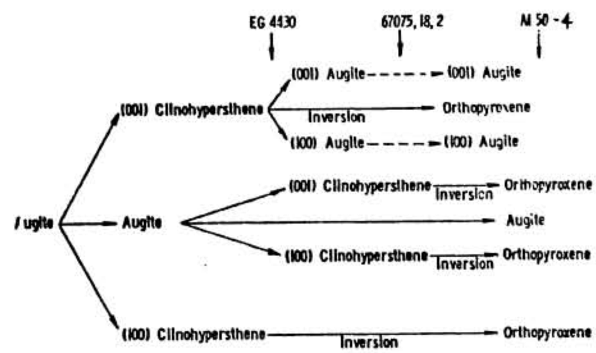

Fig. 1b. Generalized scheme of exsolution and inversion in relatively slowly cooled augites. The positions of augites from EG 4430, 67075, and M 50 in the scheme are shown approximately.

PLUTONIC AND METAMORPHIC PYROXENES

McCallum, I. S. et al.

Apollo 17 sample 77017,81 is a poikiloblastic anorthositic gabbro from the base of North Massif with ~75% plagioclase, 5% olivine, and 20% pyroxene (subequal amounts of pigeonite and augite). A late shock event has caused partial granulation. The proportions and compositions of mineral fragments in the fine grained matrix is the same as in the uncrushed areas and fragments of the primary texture are preserved, indicating that the granulation episode was not accompanied by a significant transfer of material. The mineral clasts in the matrix show shock features: undulose extinction, mosaicism, and partial shock vitrification of plagioclase. Isolated, small patches of pale brown glass occur in the matrix.

The uncrushed areas are relatively coarse grained and show a well developed poikiloblastic texture, similar in most respects to that in Apollo 16 poikiloblastic rocks. Subspherical to subhedral grains of plagioclase and olivine showing no preferred orientation are enclosed within large poikiloblasts (ca. 5mm) of pigeonite and/or augite. Where both pyroxenes occur in a single poikiloblast, they show an epitaxial relationship. Plagioclase grains contain small (<50 μm) spherical blebs of olivine and vice versa, and where plagioclase crystals are in mutual contact, polygonal grain boundaries are developed, indicative of extensive subsolidus recrystallization. This conclusion is reinforced by the compositional homogeneity of the minerals. Olivine varies from $Fo_{60.2}$ to $Fo_{63.5}$, augite from $Wo_{37.4}En_{46.2}$ to $Wo_{34.7}En_{46.4}$, and pigeonite from $Wo_{10.7}En_{58.1}$ to $Wo_{9.3}En_{61.1}$. Complete analyses of selected grains are listed in Table 2. Accessory minerals include ilmenite, troilite, Fe-Ni, and $MgAl_2O_4$ spinel.

Single crystal precession photographs of the pyroxenes indicate that the low Ca pyroxene is an untwinned pigeonite which has exsolved ~10% augite on (001). No (100) exsolution lamellae were observed and the pigeonite shows no evidence of inversion to orthopyroxene. "b" type reflections are sharp and no diffuse streaks parallel to a* are present. Cell dimensions of a typical pigeonite and its (001) augite lamellae are given in Table 1. Augite poikiloblasts show the inverse relationship, i.e., (001) clinohypersthene lamellae in an augite host. The lamellae are ~3 μm wide and resolvable in the microprobe. The data of Ross et al. (1) indicate that clinohypersthene of this composition formed at $T > 1160°C$, and the absence of inversion features imply relatively rapid subsolidus cooling. This temperature is probably close to or even above the solidus temperature of this rock.

The evidence outlined above is consistent with the following history for sample 77017: (1) brecciation, partial melting (?), and transportation of primitive anorthositic gabbro crustal material in a large impact event; (2) deposition of this material in a hot, thick ejecta blanket with little mixing of other rock types; (3) ultrametamorphism (probably accompanied by a small amount of partial melting) at $T > 1160°C$; (4) cooling to ambient temperatures at a rate sufficiently rapid to prevent inversion and yet slow enough to form 3 μm lamellae; (5) excavation by a later impact event which produced the cataclasis and the shock features.

REFERENCE: (1) Ross, M., Huebner, J. S., and Hickling, N. (1973) in Lunar Science IV, Lunar Science Institute, 637-639.

Table 1. Cell dimensions of pyroxenes

				a (Å)	b (Å)	c (Å)	β (°)	$c^*_{aug.} \wedge c^*_{pig.}$ (°)
67075,18	1	pig.	host pig.	9.66(2)	8.93(2)	5.21(2)	108.67(8)	1.33
			inverted pig.	18.30(4)	8.93(2)	5.21(2)	90	
			(001) aug.	9.74(2)	8.93(2)	5.25(2)	105.80(8)	
			(100) aug.	9.74(2)	8.93(2)	5.21(2)	105.75(8)	
			(100) pig/(001) aug.	9.66(2)	8.93(2)	5.21(2)	109.04(8)	
			epitaxial opx	18.3(1)	8.93(2)	5.21(4)	90	
	2	aug.	host aug.	9.74(2)	8.94(2)	5.24(2)	105.96(8)	1.17
			(001) pig.	9.68(2)	8.94(2)	5.22(2)	108.88(8)	
			inverted pig.	18.31(4)	8.94(2)	5.22(2)	90	
			(100) pig.	9.66(2)	8.94(2)	5.24(2)	109.29(8)	
77017,54,10			host pig. I	9.63(2)	8.88(2)	5.20(2)	108.3(5)	
			host pig. II	9.65(2)	8.88(2)	5.20(2)	109.0(5)	
			(001) aug. I	9.73(2)	8.88(2)	5.27(2)	106.2(5)	
			(001) aug. II	9.73(2)	8.88(2)	5.27(2)	106.2(5)	

Table 2. Selected microprobe analyses of pyroxenes and olivines

	1	2	3	4	5	6	7	8	9	10	11	12	13	14	15
SiO_2	51.60	49.29	51.50	53.23	53.40	49.36	49.62	51.71	52.89	51.47	51.95	51.84	52.65	52.20	36.49
TiO_2	0.39	0.49	0.22	0.15	0.29	0.76	0.67	0.21	0.33	0.15	0.39	1.26	0.77	0.85	0.05
Al_2O_3	1.05	0.88	0.41	0.56	0.88	0.40	1.19	0.36	0.56	0.77	1.80	1.97	0.67	0.94	0.00
Cr_2O_3	0.33	0.20	0.12	0.11	0.26	0.13	0.30	0.09	0.20	0.18	0.43	0.64	0.28	0.36	0.04
FeO	15.79	23.70	27.57	23.24	8.46	33.09	16.42	21.42	11.86	28.62	12.15	10.78	20.86	17.97	33.73
MnO	0.30	0.43	0.59	0.42	0.22	0.61	0.29	0.56	0.22	0.47	0.29	0.21	0.34	0.30	0.32
MgO	13.86	11.01	16.69	21.49	14.69	12.67	9.97	16.90	12.67	17.16	12.14	15.53	21.17	20.69	29.06
CaO	16.50	11.48	3.04	0.82	22.53	1.60	19.53	1.02	21.63	0.89	20.92	17.61	2.24	4.38	0.18
Na_2O	0.02	0.02	0.00	0.00	0.02	0.01	0.02	0.01	0.03	0.00	0.04	-	-	-	-
	97.83	97.53	100.05	100.03	100.75	98.17	98.02	100.79	100.40	99.71	100.12	99.84	98.98	97.69	99.87
Cation Proportions to 3 oxygens															4 Oxygens
Si	0.981	0.936	0.992	0.995	0.986	0.995	0.976	0.996	0.994	0.992	0.979	0.966	0.989	0.988	1.006
Ti	.006	.007	.003	.002	.004	.004	.010	.003	.005	.002	.006	.018	.011	.012	.001
Al	.024	.021	.009	.012	.019	.010	.028	.008	.013	.018	.040	.043	.015	.021	.000
Cr	.005	.003	.002	.002	.004	.002	.005	.001	.003	.003	.006	.009	.004	.005	.001
Fe	.251	.396	.444	.363	.131	.558	.270	.473	.186	.461	.192	.168	.328	.284	0.778
Mn	.005	.007	.008	.007	.004	.010	.005	.009	.004	.008	.005	.003	.005	.005	.008
Mg	.393	.328	.479	.599	.405	.381	.292	.485	.355	.493	.341	.431	.593	.584	1.194
Ca	.336	.246	.063	.017	.446	.035	.412	.021	.435	.018	.423	.352	.043	.089	.005
Na	.001	.001	.000	.000	.001	.001	.001	.000	.001	.000	.001	-	-	-	-
Wo	34.29	25.34	6.36	1.68	45.44	3.56	42.26	2.14	44.58	1.90	44.24	36.98	4.66	9.27	Fa 39.44
En	40.09	33.83	48.59	61.20	41.24	39.12	30.02	49.51	36.34	50.68	35.71	45.35	61.40	61.00	Fo 60.56
Fs	25.62	40.84	45.05	37.12	13.32	57.32	27.72	48.35	19.08	47.43	20.06	17.67	33.94	29.72	

1. 67075,50,01, Augite macrocrystal - bulk analysis. 2. 67075,50,34, Subcalcic augite macrocrystal - bulk analysis. 3. 67075,50,36, Inverted pigeonite macrocrystal - bulk analysis. 4. 67075,50,25,02, (001) low Ca pyroxene exsolution lamellae. 5. 67075,50,25,03, Augite host adjacent to 4. 6. 67075,50,34,16, (001) low pyroxeneexsolution lamellae 7. 67075,50,34,13, Augite host adjacent to 6. 8. 67075,50,36,8, low Ca pyroxene host. 9. 67075,50,36,13, (001) augite exsolution lamellae adjacent to 8. 10. 67075,50,39,11. (001) low Ca pyroxene exsolution lamellae. 11. Augite host adjacent to 10. 12. 77017,81, Augite 13. 77017,81, Pigeonite, 3 um beam, average of 4 points. 14. 77017,81, Pigeonite 20 um beam, representing bulk analysis before exsolution, average of 8 points. 15. 77017,81, Olivine.